Photosystem II Proteins PsbL and PsbJ Regulate Electron Flow to the Plastoquinone Pool†

Itzhak Ohad,‡ Cristina Dal Bosco,§ Reinhold G. Herrmann,§ and Jörg Meurer*,§

Department of Biological Chemistry and Minerva Center of Photosynthesis Research, The Hebrew University of Jerusalem, Jerusalem 91904, Israel, and Ludwig-Maximilians-Universität München, Department Biologie I, Botanik, Menzingerstrasse 67, 80638 München, Germany

Received May 18, 2003; Revised Manuscript Received January 6, 2004

ABSTRACT: The *psbEFLJ* operon of tobacco plastids encodes four bitopic low molecular mass transmembrane components of photosystem II. Here, we report the effect of inactivation of *psbL* on the directional forward electron flow of photosystem II as compared to that of the wild type and the *psbJ* deletion mutant, which is impaired in PSII electron flow to plastoquinone [Regel et al. (2001) *J. Biol. Chem. 276*, 41473−41478]. Exposure of Δ*psbL* plants to a saturating light pulse gives rise to the maximal fluorescence emission, Fm_L, which is followed within 4−6 s by a broader hitherto not observed second fluorescence peak in darkness, Fm_D. Conditions either facilitating oxidation or avoiding reduction of the plastoquinone pool do not affect the Fm_L level of Δ*psbL* plants but prevent the appearance of Fm_D. The level of Fm_D is proportional to the intensity and duration of the light pulse allowing reduction of the plastoquinone pool in dark-adapted leaves prior to the activation of PSI and oxidation of plastoquinol. Lowering the temperature decreases the Fm_D level in the Δ*psbL* mutant, whereas it increases considerably the lifetime of $Q_A^{\bullet-}$ in the Δ*psbJ* mutant. The thermoluminescence signal generated by $Q_A^{\bullet-}/S_2$ charge recombination is not affected; on the other hand, charge recombination of $Q_B^{\bullet-}/S_{2,3}$ could not be detected in Δ*psbL* plants. PSII is highly sensitive to photoinhibiton in Δ*psbL*. We conclude that PsbL prevents reduction of PSII by back electron flow from plastoquinol protecting PSII from photoinactivation, whereas PsbJ regulates forward electron flow from $Q_A^{\bullet-}$ to the plastoquinone pool. Therefore, both proteins contribute substantially to ensure unidirectional forward electron flow from PSII to the plastoquinone pool.

Photosystem II (PSII),[1] the oxygen evolving supramolecular pigment−protein complex of thylakoid membranes, consists of plastid and nuclear encoded proteins (*2*). The primary organization of PSII with more than two dozen subunits has been basically conserved from cyanobacteria to higher plants, although differences in subunit composition, especially of the antenna, the water splitting systems, and other peripheric subunits have arisen during evolution (*3*−*7*).

The structures of the predominant dimeric form of the PSII complex from a thermophilic cyanobacterium has been resolved at 3.7 Å by X-ray crystallography (*8*) and that of chloroplasts at 8 Å by high-resolution electron microscopy (*9*−*11*). However, the unambiguous assignment of at least 12 resolved transmembrane helices in the complex of higher plants (*12*) and six helices in the cyanobacterial PSII (*8*) remains to be established. Candidates for the unassigned transmembrane helices of the PSII complex include various low-molecular mass (LMW) subunits of largely unknown function (*1*, *13*, *14*). Many, if not all, LMW subunits are not directly involved in linear photosynthetic electron transport, but several members, such as cytochrome b_{559} (cyt b_{559}) or PsbJ, have been shown to transfer electrons or control electron flow within PSII, respectively. Inactivation of these genes and those encoding other LMW subunits often resulted in reduced photoautotrophic growth and even loss of the PSII complex (reviewed in ref *6*).

Light absorption by PSII induces charge separation resulting in the formation of the primary $P680^{\bullet+}/Phe^{\bullet-}$ radical pair followed by the reduction of the primary and secondary electron acceptor quinones Q_A and Q_B and oxidation of water via the PSII electron donor side, the manganese cluster (*15*−*17*). Upon two consecutive charge separation events, the Q_B quinone is doubly reduced, protonated, and subsequently released into the plastoquinone pool (*18*, *19*). The Q_A and Q_B sites are formed by the DE loops of the D2 and D1

† Grant supports awarded to R.G.H. and J.M. by the German Science Foundation (SFB-TR1), to R.G.H. by the Fonds der Chemischen Industrie, and to I.O. by the Israel Science Foundation (ISF) administered by the National Academy of Sciences are gratefully acknowledged.

* Corresponding author. E-mail: meurer@botanik.biologie.uni-muenchen.de. Fax: (++49)-89-1782274. Tel.: (++49)-89-17861288.

‡ The Hebrew University of Jerusalem.

§ Ludwig−Maximilians−Universität München.

[1] Abbreviations: A830, absorbance changes at 830 nm; chl, chlorophyll; cyt, cytochrome; DCMU, 3-(3′,4′-dichlorophenyl)-1,1′-dimethylurea; DCBQ, 2,6-dichloro-*p*-benzoquinone; F_o, minimal chl *a* fluorescence; Fm, maximal chl *a* fluorescence; Fm_L Fm_D, maximum chl *a* fluorescence during a short saturating light pulse and following in darkness after the pulse cessation, respectively; FR, far red light; MV, methyl viologen; Pheo, pheophytine; PSI and PSII, photosystem I and II, respectively; P680 and P700, reaction center of PSII and PSI, respectively; PQ, plastoquinone; PQH_2, plastoquinol; Q_A and Q_B, primary and secondary electron acceptor quinones of PSII, respectively; $S_{2,3}$, oxidation states of the electron donor manganese cluster; TL, thermoluminescence; Tyr_Z, Tyrosin 161 residue of the D1 protein.

10.1021/bi0348260 CCC: $27.50
Published on Web 02/07/2004

proteins of the PSII reaction center, respectively (*8*, *20*, *21*). The redox potential increases in the order $Q_A < Q_B < PQ$ (*22*), while the plastoquinone binding affinities at the Q_B site decrease in the order $Q_B^{\bullet-} > Q_B > Q_BH_2$, and thus prevent both release of the plastosemiquinone radical anion as well as back flow of electrons from PQH_2 to Q_A via reduced Q_B (*23*). Depending on the preillumination history of the plant, this one-way electron flow prevents closure of PSII at subsaturating light intensities or in darkness due to metabolic reduction of plastoquinone (*24*, *25*). However, severe heat stress has been reported to induce partial disconnection of PSII subunits as well as structural alterations at the cofactor level (*26*, *27*) that leads to back electron flow from the reduced plastoquinone pool and reduction of Q_A (*22*, *28*−*32*). Reduction of plastoquinone in darkness attributed to stromal electron donors accumulated during illumination has also been observed, especially in C_4 plants after illumination with actinic light (*33*−*36*). However, this does not a priory imply that the reduced plastoquinone pool in darkness reduces Q_A.

Cotranscription of the four genes of the highly conserved *psbEFLJ* operon encoding bitopic LMW proteins of PSII suggests that the functions of proteins encoded by these genes are interrelated (*37*). Selective inactivation of each of the individual LMW subunits of this operon in tobacco resulted in specific PSII impairments (*13*). Selective inactivation of the *psbE* or *psbF* genes encoding subunits α and β of the cyt b_{559}, respectively, has been reported to cause loss of PSII stability in cyanobacteria (*38*), *Chlamydomonas* (*13*, *39*), as well as in tobacco (*13*). Cyt b_{559} could play a protective role against oxidative stress by mediating cyclic electron flow from $Q_B^{\bullet-}$ and $Q_A^{\bullet-}$ back to the manganese cluster (*40*−*44*). Depending on the pH, photooxidized cyt b_{559} is reduced either by plastoquinol or via $Q_B^{\bullet-}$ in darkness (*45*, *46*).

The *psbL* gene encodes a PSII polypeptide of 4.3 kDa that contains a single transmembrane helix (*47*). Presently, the role ascribed to PsbL in cyanobacterial PSII is mostly based on in vitro studies in which the isolated PSII core complex depleted of plastoquinone and PsbL protein after detergent treatment was reconstituted with lipids, quinones, and isolated PsbL proteins (*48*−*51*). Inactivation of *psbL* in *Synechocystis* led to a reduction of PSII reaction centers to about 25% of the normal level, demonstrating the importance of this LMW component in vivo (*52*).

In tobacco, both PsbL and PsbJ are not required for assembling monomeric PSII complexes (*13*, *53*). However, the tobacco Δ*psbJ* mutant exhibits a phenotype drastically impaired in the electron flow to the plastoquinone pool (*1*) and possibly affects the donor side activity of PSII as well (*53*). In this work, based on fluorimetric, thermoluminescence, and absorbance measurements, we demonstrate that PsbL is not required for water splitting, primary charge separation, electron flow within PSII, and reduction of the plastoquinone pool. Furthermore, we provide evidence for the role of PsbL in preventing back electron flow from PQH_2 and closing of the reaction center of PSII even in complete darkness. Thus, the presence of PsbJ and PsbL promote unidirectional electron flow from PSII to the PQ pool.

MATERIALS AND METHODS

Plant Material. The Δ*psbL* and Δ*psbJ* tobacco mutants as well as control plants which contain the *aadA* cassette in a neutral EcoRV (RV) site, here referred to as wild type, were generated and grown on selective spectinomycin-supplemented medium as described (*1*, *13*). Initially, various independent transformants that have been isolated and analyzed displayed comparable light sensitivity, variable Fv/Fm ratios in different leaves or leaf areas, a high Fo type fluorescence, and unusual fluorescence decay kinetics showing a second fluorescence raise in darkness (Fm_D) after shutting off the exciting light pulse. Regenerants of two independent shoots were selected and propagated for this study. PCR and Southern analysis demonstrated that the *aadA* cassette was inserted into the expected site of the chloroplast genome (*13*). Mutant plants did not grow photoautotrophically, and leaves senesced within a few weeks.

Measurements of Photosynthetic Activity. PSII of Δ*psbL* mutants is highly unstable, and its activity is completely lost upon isolation of thylakoids even under gentle conditions resulting in the disappearance of any variable fluorescence. Therefore, we could not use isolated mutant membranes for the analyses and consequently employed noninvasive methods for assaying the activity of detached leaves using fluorescence kinetics (*1*, *54*). However, oxygen evolution could be measured in isolated thylakoids obtained from Δ*psbJ* leaves and was found to be about 20−30% of that exhibited by wild type thylakoids (*1*). Fluorescence emission of both Δ*psbL* and Δ*psbJ* leaves was measured by the pulse amplitude modulated fluorimeter (PAM-101, Walz, Effeltrich, Germany). Fluorometric inspection revealed a gradual loss of PSII activity with age of Δ*psbL* plants. Apparently, about 85−95% of older but still green mutant leaves lost PSII activity completely during growth even at low light intensity. Approximately 250 leaves of Δ*psbL* mutant plants with residual PSII activity were selected among which only 45 showed significant PSII activity (Fv/Fm >0.2). Often, parts of the same leaf exhibited activity while other parts had lower or no detectable PSII activity and emitted high fluorescence.

Variable fluorescence was measured by modulated weak 650 nm light pulses (0.01 μE m^{-2} s^{-1}) delivered at 1.6 kHz at the leaf surface. At this low light intensity, electron flow via PSII does not generate accumulation of reduced Q_A, and the fluorescence level, Fo, which depends largely on the organization of chlorophyll molecules and closure of PSII, is low. Short pulses (1 s) of white light emitted by tungsten halogen lamps (4.000 μE m^{-2} s^{-1}) saturate PSII electron flow reducing Q_A and cause maximal fluorescence emission (Fm). Subsequent fluorescence decay in darkness reflects the oxidation of $Q_A^{\bullet-}$ as measured by modulated weak light pulses. The variable fluorescence (Fv) characteristic of active PSII is expressed as the difference between Fm and Fo. The fluorescence induction traces shown in most figures are normalized to equal heights of the Fv level. Far-red light (FR, 710 nm) was supplied by the PAM-PSI attachment at intensities between 3 and 9 Wm^{-2} at the leaf level, as measured by a YSI-Kettering Radiometer model 65A. Detached and infiltrated leaves were kept on wet Whatman filter paper in Petri dishes at room temperature in darkness for up to several hours. All measurements were carried out on leaves dark-adapted for at least 10 min. For low-temperature experiments, leaf disks (1 cm diameter) were excised and placed in a temperature-controlled measuring cuvette.

DCMU, DCBQ (both 100 μM in 1% methanol), or MV (1 mM) were vacuum infiltrated into intact leaves or leaf disks or leaves were incubated on filter paper in the previous solutions for up to 1 h in strict darkness. Anaerobic conditions were generated by placing the leaves in a screw-caped glass vial (3 mL) containing 0.5 mL of water and flushing the vial for 3−4 min with pure argon at room temperature. The vial was rapidly closed and kept in darkness, and fluorescence kinetics was measured by placing the fiber optic of the PAM 101 apparatus directly on the anaerobic vial containing the leaf.

The temperature-dependent light emission (thermoluminescence, TL) due to charge recombination of $Q_B^{\bullet-}/S_{2,3}$ or $Q_A^{\bullet-}/S_2$ states in the absence or presence of DCMU, respectively, was measured as described (*55*−*57*). Leaves (0.8−1.5 cm) were dark-adapted on the thermoluminescence apparatus stage at 20 °C for 3 min followed by cooling to 0.5−1 °C. Since PSII is inactivated by freezing, excitation of the leaf by a xenon discharge lamp delivering single turnover flashes of 3 μs was carried out at 0.5−1 °C. To obtain maximal photon emission, measurements started immediately after excitation by two consecutive light flashes (*55*) delivered by a EG&G lamp 0.05 mF capacitor, charged at 1.000 V. The samples were heated at a constant rate (0.5 °C/s), and light emission was measured by photon counting.

The activity of PSI was assayed by measuring light induced absorption changes at 830 nm using the PAM-101 PSI attachment (*58*). The redox level of P700 has been recorded in the steady state at 20 μE m^{-2} s^{-1} white light. Following switching off the actinic light, P700 was fully reduced, and FR light was applied to record the maximal oxidized state of P700. Light pulses of 1 s duration and 4.000 μE m^{-2} s^{-1} intensity were used to estimate PSII dependent reduction of P700 in background FR light. Subsequently, light pulses were given in darkness to follow the PSII independent oxidation of PSI.

RESULTS

ΔpsbL Mutant Is Highly Light Sensitive. Fluorimetric measurements uncovered that residual PSII activity in green Δ*psbL* leaves varied greatly and depended critically on leaf development and light intensity during growth. The Fv/Fm ratio ranged from 0 to about 0.45 without notable effect on leaf morphology and pigmentation. The fraction without PSII activity (Fv = 0) constituted the majority of green leaves. Immunological analysis showed that the presence, absence, and amount of PsbJ in Δ*psbL* are clearly related with the occurrence and extent of PSII activity (Figure 1A). In green Δ*psbL* leaves with PSII activity {Fv/Fm ratios >0.2 [Δ*psbL* (+)]}, PsbJ was clearly detectable but barely detectable or absent in those with low PSII activity {Fv/Fm ratios < 0.05 [Δ*psbL* (−)]} (Figure 1A). This refined approach explains why in our previous work we did not detect PsbJ in unselected Δ*psbL* green leaves (*13*). Expectedly, PsbJ was missing in Δ*psbJ* leaves even when these were selected for the highest PSII activitiy (Fv/Fm ratios >0.3; Figure 1A). Levels of PsbE and PsbA (α-subunit of cytochrome b_{559} and D1 protein of PSII, respectively) were also significantly reduced in plants with low PSII activity, while levels of the NDH complex and of the ATP synthase, as judged from immunoblot data with anti-NdhH and anti-atpD-antibodies, respectively, remained unaffected. Although levels of PsbE and PsbA are low in mutant leaves (~10% of the wild type), the proteins are assembled into a functional complex capable of transferring electrons to the plastoquinone pool leading to a relatively high PSII activity (up to 50% of the wild type).

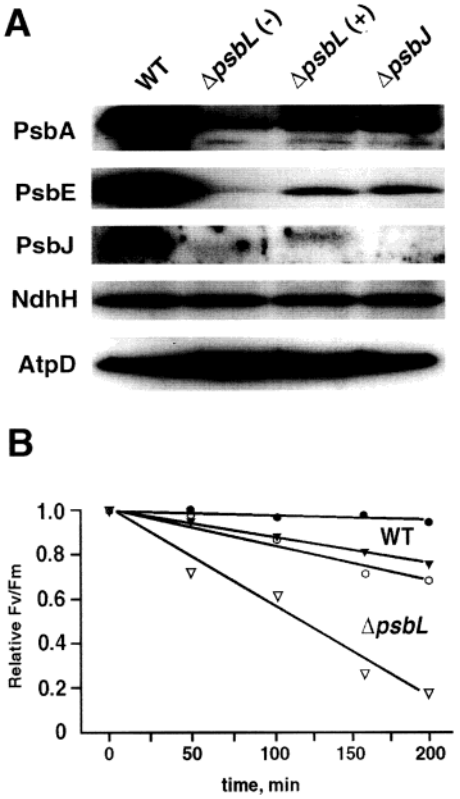

FIGURE 1: Light sensitivity of PSII in the Δ*psbL* mutant. (A) Immunological analysis of wild type and mutant leaves with different PSII activities. Mutant leaves were selected with F_v/F_m ratios >0.2 [Δ*psbL* (+)] and with Fv/Fm ratios of < 0.05 [Δ*psbL* (−)] and subjected to immunoblot analysis using antibodies raised against the PSII subunits PsbA, PsbE, and PsbJ as well as subunit NdhH and AtpD of the NAD(P)H dependent dehydrogenase and the ATP synthase, respectively. (B) Time course of PSII photoinactivation in wild type (plain symbols) and Δ*psbL* leaves (open symbols) (Fv/Fm >0.2) exposed to 100 μE m^{-2} s^{-1} for 3 h in the absence (circles) or presence of chloramphenicol (200 μg mL^{-1}) (triangles). The results are expressed as % of the initial Fv/Fm values prior to light incubation.

Light exposure of Δ*psbL* leaves exhibiting Fv/Fm levels equal to or higher than 0.2 resulted in 80% inactivation of PSII within 3 h at only 100 μE m^{-2} s^{-1} if chloramphenicol was added to prevent recovery of PSII activity by inhibiting de novo synthesis of the reaction center D1 protein (*59*). Under these conditions, only a 20% loss of PSII activity occurred in the wild type leaves (Figure 1B). However, in absence of the inhibitor, loss of PSII activity was only 30% in the mutant, indicating that the light induced damage can be repaired by the mutant plastid to a large extent (~50%) even at this light intensity that is 10-fold higher than that used for plant growth (Figure 1B).

Thus, regions of leaves exhibiting variable fluorescence contain PSII complexes that are not photodamaged or the light-induced phortodamage has been repaired. Low Fv/Fm values in various leaves or leaf segments could be the results of the presence of closed or irreversibly damaged centers that contribute to a high Fo level. As compared with the wild type, PSII of the Δ*psbL* mutant is considerbly more

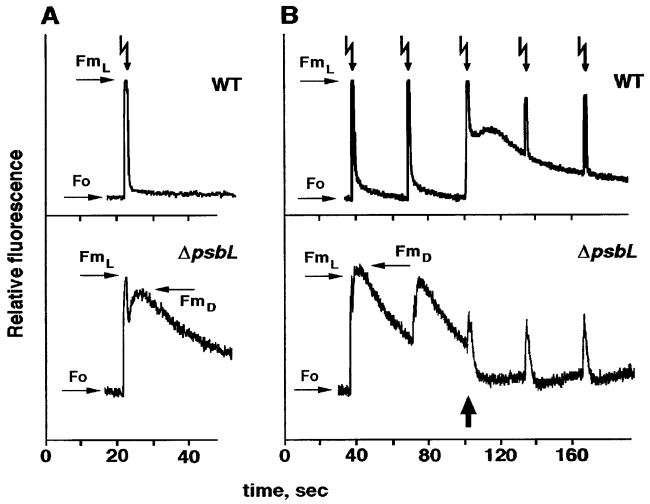

FIGURE 2: Fluorescence induction kinetics of control and Δ*psbL* mutant leaves. Fluorescence induction traces induced by saturating white light pulses (squiggled arrow) show the maximal fluorescence raise during the light pulse (Fm_L) and the second raise after the pulse, in darkness (Fm_D). The Fv_L ($Fm_L - F_o$) levels were normalized to equal heights. (A) Traces showing the fluorescence rise and decay of dark-adapted leaves of wild type and Δ*psbL* mutant exposed to a 1 s light pulse; the Fv_L/Fm_L ratio of the wild type is 0.79; the Fv_L/Fm_L and Fv_D/Fm_D [$(Fm_D - Fo)/ Fm_D$] of the mutant calculated from the original traces are 0.46 and 0.42, respectively. (B) Fluorescence induction traces of dark-adapted leaves exposed to two consecutive saturating light pulses followed by application of continuous actinic light (upward heavy arrow) and three additional pulses; note that the actinic light induces an initial transient raise of the wild type steady state fluorescence caused by an increase in the plastoquinol level, whereas the fluorescence is rapidly quenched in the mutant. The actinic light suppresses Fm_D. The calculated Fv_L/Fm_L, Fv_D/Fm_D of the mutant, and Fv_L/Fm_L of the wild type are 0.28, 0.30, and 0.79, respectively.

sensitive to light; thus, over a period of 2−3 weeks of growth and light exposure, a larger proportion of the PSII population is irreversibly damaged, and its proteins degraded as indicated by the low levels of the PSII proteins detected by immunoblotting in leaves exhibiting Fv/Fm values <0.2 (Figure 1 A).

*Δ*psbL *Mutant Exhibits an Unusual PSII Fluorescence Kinetics*. It is widely accepted that variable fluorescence is linearly related to PSII activity (*26*, *27*, *54*). Measurements of $Q_A^{\bullet-}$ oxidation in Δ*psbL* leaves exhibited an unexpected fluorescence decay pattern as compared to the control. In wild type, the Fm level elicited by the short saturating light pulse, designated Fm_L (L, for light), decayed rapidly in darkness to the original Fo level (Figure 2A). Following the Fm_L fluorescence rise due to the light pulse in Δ*psbL*, the fluorescence decayed after the pulse within 300−400 ms at a rate comparable to that of the control leaves but, surprisingly, increased again in darkness resulting in an unexpected second maximum fluorescence level, designated as Fm_D (D, for dark) (Figure 2A). This second fluorescence peak decayed slowly (up to 2 min to reach the previous Fo level) (Figure 2A and data not shown). Fm_D was detected in all mutant leaves exhibiting variable fluorescence activity. The appearance of Fm_D several seconds after the exciting light pulse is specific for the Δ*psbL* mutant and has not been observed in any other PSII mutant or stressed wild type leaves.

The Fo level and Fv/Fm were identical in wild type plants grown under autotrophic conditions or on medium supplemented with sucrose. In both mutant and wild type, application of FR light at different light intensities did not lower the dark Fo level, indicating that the PQ pool in dark-adapted leaves was not reduced in darkness by metabolic activity (data not shown). Therefore, we conclude that the difference between the control and the Δ*psbL* leaves are due to differences in PSII properties.

The ratio Fm_D/Fm_L generated by a saturating light pulse of 1 s varied between 0.6 and 1.0 and occasionally reached values up to 1.2. The latter was only observed in Δ*psbL* leaves with very low PSII activity. The Fm_D peak could be detected only in dark-adapted mutant leaves and in all leaves exhibiting residual PSII activity. After continuous illumination even with weak light or after multiple consecutive saturating light pulses of 1 s, its appearance was prevented (ref *13* and data not shown). The mutant leaves exhibited rapid fluorescence quenching upon exposure to continuous 650 nm light (Figure 2B) or white actinic light (not shown) that can be ascribed to the high energy quenching component (q_E) of nonphotochemical quenching (NPQ) and to rapid light induced oxidation of the plastoquinone pool (photochemical quenching) that allows PSII centers to be reoxidized (Figure 2B). As will be shown next, the ratio of PSI/PSII activity in Δ*psbL* mutants is high; thus, in continuous actinic light, PSI activity surpasses that of PSII.

Contribution of Inactive Centers to the Fm_L Peak. To evaluate to what extent the presence of inactive and disassembled PSII complexes in leaf areas containing both active and inactive PSII affects the measured kinetics, we determined their possible contribution to the obtained thermoluminescence and variable fluorescence signals (Figure 3). We examined inactive mutant leaves that did not display variable fluorescence that were, however, similar in size and chlorophyll content to mutant leaves that exhibited PSII activity (Fv/Fm >0.2). Since disassembled or functionally inactive PSII centers do not perform electron flow from the PSII donor to the acceptor side, such leaves expectedly did not contribute to the thermoluminescence A and B signals (data not shown).

The Fo type of fluorescence (i.e., absence of a variable fluorescence component) increased significantly in the green leaves containing mostly nonactive PSII (Fv ∼0). However, in those leaves, the saturating light pulse elicited a small rapid lowering of the fluorescence signal that returned to the Fo baseline upon cessation of the light pulse (Figure 3). Therefore, the presence of inactive centers in leaf areas containing heterogeneous PSII centers contributes to the measured variable fluorescence but only by lowering the recorded fluorescence intensity (Fm_L*) elicited during the saturating light pulse (Fm_L* < Fm_L). This phenomenonon provides a reasonable explanation for the fact that Fm_D occasionally exceeds Fm_L (Figure 2B). Under such conditions, the observed Fm_L levels cannot be precisely measured because they are superimposed by the negative contribution of inactive centers.

Appearance of Fm_D Is Temperature Dependent. Recently, we have reported that fluorescence decay after a saturating light pulse ascribed to oxidation of $Q_A^{\bullet-}$ via Q_B electron flow to the PQ pool in Δ*psbJ* plants shows a very slow kinetics ($t_{1/2}$ ∼30−60 s). Thermoluminescence measurements indicated that the oxidation of $Q_A^{\bullet-}$ in this mutant occurs mostly via back electron flow within PSII to the oxidized manganese cluster of the water oxidation system (*1*).

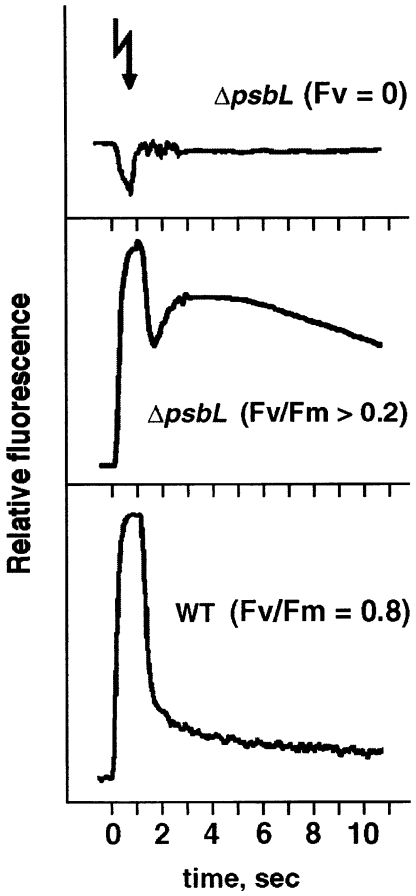

FIGURE 3: Contribution of inactive centers to Fm_L in Δ*psbL* mutant leaves. Fluorescence traces induced by a single light pulse of 1 s in mutant leaves without (Fv = 0) and with (Fv/Fm >0.2) PSII activity and wild type leaves (Fv/Fm = 0.8).

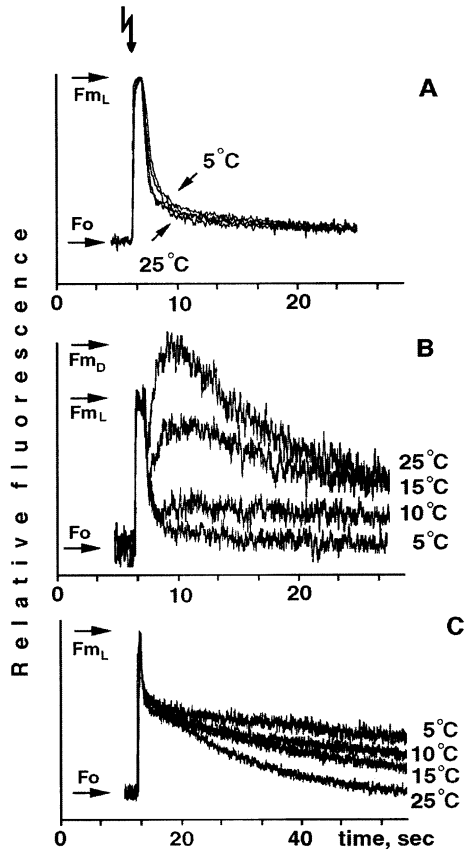

FIGURE 4: Fluorescence induction kinetics as a function of temperature. Dark-adapted leaves of control and mutant plants were incubated at temperatures as indicated, then exposed to single (1 s) pulses of saturating light (squiggled arrow), and the fluorescence transients were recorded. The Fv_L values (Fm_L − Fo) are normalized to equal heights. (A) control leaves; (B) Δ*psbL* leaves; and (C) Δ*psbJ* leaves.

The back electron flow from $Q_B^{\bullet -}$ to the oxidized Mn cluster demands a relatively high activation energy and thus is strongly temperature dependent (*60*). Therefore, we compared the temperature dependency of the fluorescence decay kinetics exhibited by Δ*psbL* and Δ*psbJ* to that of control leaves (Figure 4). No significant temperature effect was observed in the Fm_L and Fo levels, nor in the fluorescence decay kinetics of control leaves (Figure 4A). Lowering the temperature did not change the initial kinetics of fluorescence decay in Δ*psbL* leaves, indicating that oxidation of $Q_A^{\bullet -}$ and forward electron flow occur in the mutant. However, the appearance of the Fm_D peak was progressively lost with decreasing the temperature and abolished at 5 °C (Figure 4B). These results suggest that after a light saturating pulse, decay of Fm_L is altered in the Δ*psbL* mutant probably due to the temperature-dependent reduction of PSII in darkness by back electron flow from the reduced plastoquinone pool generating the Fm_D fluorescence peak. The temperature effect on Fm_D was fully reversible in the same leaf when the temperature was shifted back to 25 °C (data not shown), indicating that PSII was not harmed by the experimental procedure. Since in the Δ*psbJ* mutant oxidation of $Q_A^{\bullet -}$ occurs via energy dependent back electron flow inside PSII, lowering the temperature resulted in a significant increase in the fluorescence decay time (Figure 4C).

Working Hypothesis: Fm_D Is Generated by Back Electron Flow to Q_A from the Reduced Plastoquinone Pool in Darkness. The data presented so far suggested that the absence of subunit PsbL results in an assembly of PSII in which the Q_B site is altered. The altered site permits electron flow from reduced plastoquinol generated during the saturating light pulse to Q_A. To test the possibility that the observed effects of the Δ*psbL* mutation are related to the ratio PQH_2/PQ of the plastoquinone pool, several experiments were carried out to show that Fm_D depends on the extent of PQ reduction. The Fm_D appearance was examined relative to the PQ reduction state, which was modified by (a) application of actinic pulses of different intensities and durations, (b) inhibition of Q_B reduction by DCMU or artificial electron acceptors such as DCBQ, and (c) oxidation of plastoquinone by O_2 or PSI activity.

Effect of PQ Pool Reduction. Given that the reduction of Q_A can be achieved by a saturating light pulse shorter than 1 s, whereas accumulation of reduced plastoquinol requires longer illumination times, one would expect that the appearance of Fm_D will be related to the duration of the light pulse. Using a single 50 ms flash allowing only a few turnovers of PSII, neither the maximal fluorescence level, Fm_L, nor the appearance of Fm_D were elicited in Δ*psbL* (Figure 5A). Exposing dark-adapted leaves to light pulses of 0.2 s induced the Fm_L response and the appearance of a low Fm_D. A maximum Fm_D level appeared at saturating light pulses of 0.6 s duration. Increasing the intensity of the pulse from 100 to 1.000 μE m^{-2} s^{-1} at a constant duration of 1 s resulted in

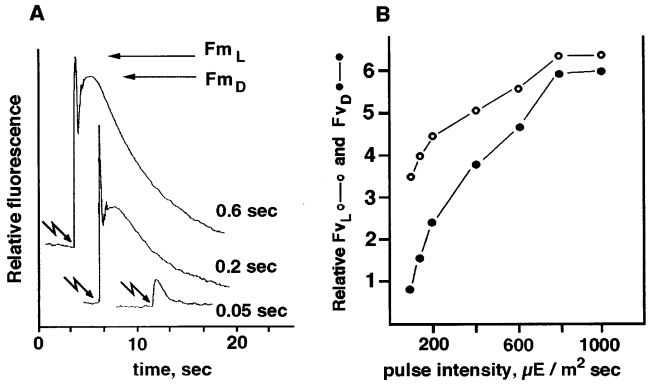

FIGURE 5: Effect of the light pulse duration and intensity on the appearance of the Fm_L and Fm_D fluorescence peak. (A) Leaves of the Δ*psbL* plants were exposed to saturating light pulses of different duration. The traces before the application of the light pulse (squiggled arrow) do not represent the real value of Fo relative to the height of Fm. (B) Calculated levels (relative units) of Fv_L and Fv_D from traces obtained by exposing the leaves to light pulses of 1 s at different intensities; the Fv_L/Fm_L of the leaf exposed to a saturating light pulse of 1 s calculated from the recorded trace was 0.22.

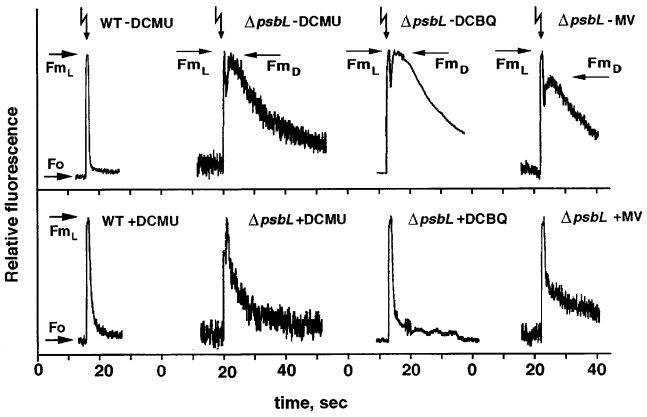

FIGURE 6: Effect of DCMU, DCBQ, and MV on the Fm_D fluorescence peak in Δ*psbL* mutant leaves. Fluorescence induction kinetics was measured in the absence or presence of Q_B reduction inhibitors DCMU or DCBQ or MV, an electron acceptor of PSI. Note that Fm_D appearance is abolished under all conditions preventing accumulation of reduced plastoquinone during the 1 s saturating light pulse (squiggled arrow); the Fv_L values were normalized; the Fv/Fm ratios of the control leaves (left panel) were 0.78 and 0.69 before and after DCMU infiltration, respectively; the Fv_L/Fm_L ratio before infiltration of the Δ*psbL* leaves with the various chemicals were 0.41, 0.30, and 0.20 in the second, third, and fourth panels from left, respectively; after infiltration, the Fv_L/Fm_L values were lowered to 0.12, 0.18, and 0.18 in the panels, respectively.

a 2-fold increase in Fv_L but an approximately 8-fold increase in Fv_D, indicating that the appearance of Fm_D depends on the amount of reduced plastoquinone (Figure 5B).

Effect of Preventing Reduction of the PQ Pool or Oxidation of the PQH_2 Pool Formed during the Light Pulse. The working hypothesis rests on the assumption that plastoquinol reduces Q_A in the Δ*psbL* mutant. Thus, the presence of DCMU preventing reduction of Q_B or that of DCBQ, an artificial electron acceptor from PSII at the Q_B site, during the saturating light pulse should avoid reduction of the plastoquinone pool and consequently the appearance of Fm_D. Indeed, DCMU and DCBQ abolished the appearance of the fluorescence peak Fm_D after the saturating light pulse, consistent with the idea that electron flow via the Q_B site and accumulation of plastoquinol or semiquinone is essential for the formation of Fm_D (Figure 6). The fact that DCMU does not completely restore the fast decay of the fluorescence at the concentrations used (100 μM) indicates that the affinity of the Q_B site for DCMU and possibly also for plastoquinol has been altered in the Δ*psbL* mutant. This could lead to a competition of the plastoquinol with the herbicide for the binding site. Using different individual intact leaves does not allow an accurate titration of the Q_B site affinity for the herbicide. Therefore, further experiments need to be devised to allow measurements of the affinity of the altered Q_B site for DCMU as well as for other urea or phenolic type herbicides. In contrast, DCBQ completely restores the Fm_L decay kinetics as compared to DCMU, indicating that the putative alteration of the Q_B site does not prevent electron transfer to this artificial electron acceptor (Figure 6).

Effect of Plastoquinol Oxidation by PSI Electron Flow to Endogenous or Efficient Exogenous Electron Acceptors. Since prolonged illumination or exposure of dark-adapted leaves to consecutive multiple saturating light pulses of 1 s duration abolished the appearance of Fm_D, it is conceivable that electron flow due to light activation of carbon fixation oxidizes the plastoquinol pool formed during light pulses and thus prevents back electron flow to PSII in Δ*psbL* leaves (*13*). If this were the case, one would expect that conditions promoting oxidation of the plastoquinol pool should also prevent the appearance of Fm_D. In line with this assumption, infiltration of Δ*psbL* leaves with MV that efficiently accepts electrons from reduced PSI significantly lowered Fm_D emission (Figure 6).

To evaluate the involvement of plastoquinol in the appearance of Fm_D in absence of externally added inhibitors or electron acceptors, the effect of FR light preferentially exciting PSI, and thus increasing the plastoquinol oxidation rate, was measured as well. Exposure of Δ*psbL* leaves to FR light prior to the saturating light pulse prevented the appearance of Fm_D (Figure 7A). Titration of the Fm_D level as a function of the FR light intensity applied during and/or immediately after the pulse shows that Fm_D is progressively diminished with increasing FR light intensity (data not shown).

In control plants, P700 is almost reduced during steady-state illumination by actinic light intensities of 20 μE m^{-2} s^{-1} and is oxidized by FR light (Figure 7B). A saturating white light pulse causes rapid reduction of P700 due to PSII activity followed by reoxidation in the presence of FR background light. A short white light pulse delivered in absence of FR background light transiently reoxidizes P700 since under these conditions the rate-limiting reduction of P700 by PSII activity is too low as compared to the rate of P700 oxidation by the saturating light pulse. The P700 redox state of Δ*psbL* leaves that either exhibit an Fv/Fm ratio above 0.2 (Δ*psbL* +Fv) or do not display measurable variable fluorescence (Δ*psbL* −Fv) have been compared with those of the wild type. Unlike in control leaves, P700 is mainly oxidized under steady-state illumination conditions in Δ*psbL* +Fv mutant leaves. Continuous FR light rapidly oxidizes P700 that can only partially be reduced by a 1 s pulse of saturating white light on a background of FR light in the Δ*psbL* +Fv mutant leaves. FR light-induced reoxidation of P700 occurs faster in Δ*psbL* +Fv material than in wild type because PSII activity is significantly lower in the Δ*psbL* +Fv

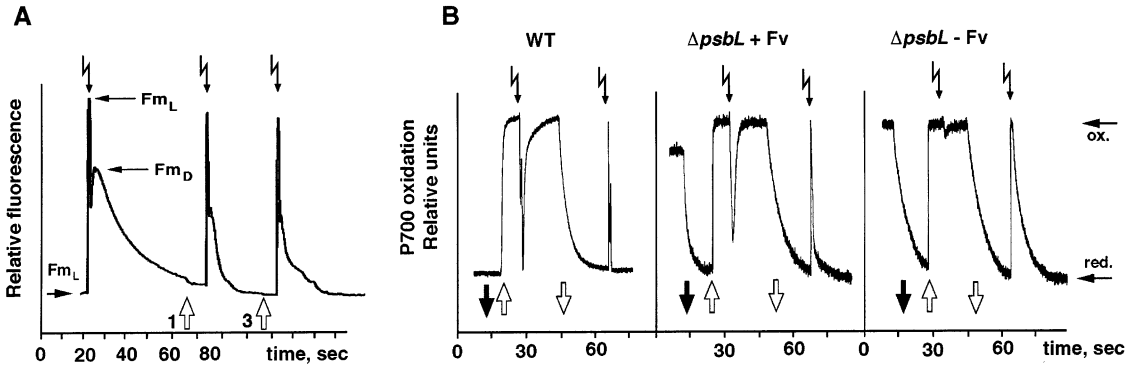

FIGURE 7: Far-red light effect on the Fm_D fluorescence emission and PSI activity of the Δ*psbL* mutants. (A) Mutant leaves exhibited both Fm_L and Fm_D fluorescence peaks upon excitation by 1 s saturating light pulse (squiggled arrow) (ratio Fv_L/Fm_L of 0.4); reexposure of the leaf to saturating light pulses on a background of FR light (upward heavy open arrows) of increasing intensity (setting 1 and 3 of the PAM PSI light emitter) lowered considerably the appearance of the Fm_D peak; (B) Control leaves and two types of young and fully green Δ*psbL* leaves were used, one exhibiting Fv_L/Fm_L variable fluorescence above 0.2 (Δ*psbL* +Fv) and another lacking completely PSII variable fluorescence activity (Δ*psbL* −Fv). The P700 oxidized state of wild type and Δ*psbL* mutant leaves exposed to actinic light was recorded. The signal level of the wild type indicating a reduced state of PSI was not affected after switching off the actinic light (downward heavy black arrow); however, the signal of the mutants was lowered upon shutting down the actinic light, indicating that PSI was significantly oxidized. Application of FR light (upward heavy open arrow) oxidized PSI in both control and mutants leaves; subsequent saturating light pulses (squiggled arrow) on the background of FR light transiently reduced PSI in control and Δ*psbL* +Fv but not in Δ*psbL* −Fv plants; saturating light pulses after switching off FR light (downward heavy open arrow) oxidized PSI in the control and both mutant leaves; ox., oxidized P700; red., reduced P700.

mutant as compared to that of the control leaf. Following the cessation of the FR light and reduction of P700, a pulse of saturating white light oxidizes P700 that again is rapidly rereduced in darkness as has been observed in control plants (Figure 7B). Expectedly, the slowest rereduction rate has been recorded in Δ*psbL* −Fv plants where P700 becomes completely oxidized by actinic background light, and no significant reduction by light pulses has been observed in background FR light (Figure 7B). These results show that functional photosynthetic electron transport components such as cyt b_6f, plastocyanin, and PSI complexes are present in mutant leaves and that loss of PSII activity is specifically due to the instability of PSII complexes lacking PsbL.

The decay of Fm_L after the saturating light pulse depends on forward electron flow from $Q_A^{\bullet-}$ via Q_B to the PQ pool and partially on back electron flow to the PSII donor side from $Q_A^{\bullet-}$ and $Q_B^{\bullet-}$ to $P680^{\bullet+}$ (*27*). Both reactions are expected to be independent of the oxygen concentration of the environment. In darkness, plastoquinol is slowly oxidized by ambient oxygen. In fact, the kinetics of the fluorescence decay in control leaves is not affected by anaerobic conditions (Figure 8). If the appearance of Fm_D in the Δ*psbL* leaves is due to back electron flow from the PQ pool, its initial level and following decay should be related to the rate of oxidation of the plastoquinol pool. Indeed, the decay of Fm_D in the Δ*psbL* mutant was significantly retarded under anaerobic conditions (Figure 8).

Charge Recombination in PSII as Detected by Thermoluminescence. Information on the function and properties of the quinone binding sites and back electron flow within PSII can be deduced from thermoluminescence measurements. $P680^{\bullet+}/Pheo^{\bullet-}$ charge recombination in the process of back electron flow from the reduced $Q_A^{\bullet-}$ or $Q_B^{\bullet-}$ semiquinones to the oxidized S-states of the manganese cluster is accompanied by light emission (*55*, *61*, *62*). Charge separation and formation of the $S_{2,3}/Q_B^{\bullet-}$ may occur following single turnover flash excitations at about 0 °C. However, back electron flow is prevented at this temperature, and the energy of activation required to overcome the redox potential barrier

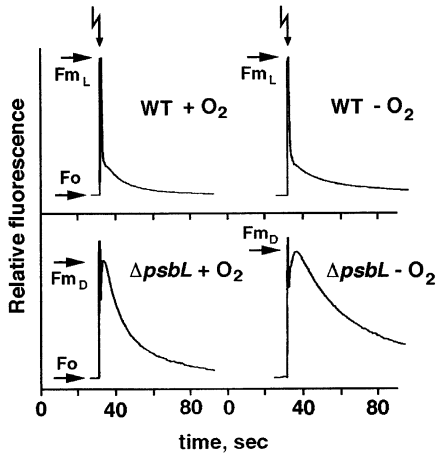

FIGURE 8: Effect of anaerobiosis on the decay of the Fm_D fluorescence peak. The fluorescence induction characteristics of dark-adapted control and mutant leaves were recorded in air (+ O_2) or argon (− O_2) atmosphere. Fv_L values were normalized. Note that absence of oxygen has no effect on the decay of fluorescence in wild type leaves but delays significantly the oxidation of the Fm_D peak in the Δ*psbL* mutant.

can be supplied by heating the sample in darkness. The temperature at which maximum photon emission occurs is related to the redox potential difference between the electron donor, $Q_B^{\bullet-}$ or $Q_A^{\bullet-}$ (the B and A bands of thermoluminescence signal, respectively), and S_2 or S_3, the oxidation states of the manganese cluster at the donor side (*55*, *63*). The A band is obtained in the presence of DCMU that prevents the oxidation of reduced Q_A via forward electron flow. The temperature of charge recombination in the presence of DCMU at about 11−13 °C is in the normal range (*55*, *64*) and is basically the same for both wild type and Δ*psbL* leaves, indicating that at least in the dark the redox potential of $Pheo^{\bullet-}$:Pheo/Q_A:$Q_A^{\bullet-}$ is not significantly altered in the mutant (Figure 9). The slight difference between the mutant A band emission temperature (Figure 9, trace 4) as compared to that of the wild type (Figure 9, trace 2) may be marginal and arise at least partially from the broadness of the wild

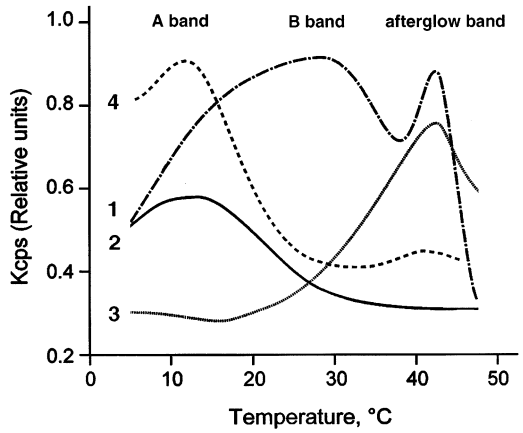

FIGURE 9: Thermoluminescence emission ascribed to charge recombination of the pairs $S_2/Q_A^{\bullet-}$ (A band) and $S_{2,3}/Q_B^{\bullet-}$ (B band) in the presence or absence of DCMU, respectively. The A band was measured in control and Δ*psbL* leaves infiltrated with 20 μM DCMU and kept for 1 h in darkness. Trace 1, control leaf showing the B band (25−35 °C) and the afterglow band (43−45 °C). Trace 2, the A band emission at about 15 °C of the control leaf (*Y* axis, 17 Kcps). Traces 3 and 4, Δ*psbL* leaves showing the afterglow band at 43−45 °C and the A band emission at about 14 °C, respectively (*Y* axis, 1 Kcps). Note that the B band at about 30 °C is absent in the mutant thermoluminescence signal trace. The emission intensity is lower in the mutant leaves due to the lower content of active PSII. The large difference in the maximal emission of the A or B bands between wild type and mutant is related to the amount of active PSII in a sample of the same size (1.5 cm diameter of the leaf disks).

type signal. Reduction of Q_A by the plastoquinol pool requires indeed electron flow uphill the potential gradient in agreement with the temperature dependency of this process (Figure 4). However, it could be possible that changes in the redox potential of $Q_A/Q_A^{\bullet-}$ occur but are offset by changes on the PSII donor side.

Control leaves exhibited a broad emission B band at about 25−30 °C and an additional minor band at about 43−45 °C that can be considered as an afterglow band (*65*). The afterglow band was detected also in mutant thermoluminescence emission. The appearance of a broader DCMU sensitive band at 43 °C in Δ*psbL* may reflect the afterglow band, again indicating that the Q_B binding site is altered in the mutant.

However, most importantly, the Δ*psbL* leaves did not emit a B band signal. The absence of the B band in the Δ*psbL* leaves strongly argues for the possibility that properties of the Q_B site are profoundly altered. This alteration can be expressed in the affinity of the site to ligands such as DCMU and possibly to the PQ semiquinone that may be released allowing access to the plastoquinone pool.

DISCUSSION

The role of the PsbL subunit in PSII has been previously investigated in vivo using a *Synechocystis* sp. PCC 6803 line in which the corresponding gene was inactivated (*52*). The mutant thylakoids contained approximately 25% of the wild type D1, and D2 protein levels on a chlorophyll basis, however, had no detectable activity of PSII, measured as oxygen evolution or quinone reduction, nor binding of DCMU. In vitro reconstitution experiments, in turn, have led to the conclusions that PsbL is required for the oxidation of Y_Z by P680 to form Y_Z^+ P680 $Pheo^-$ and located close to the donor side within the cyanobacterial PSII (*51*).

Deletion of *psbL* in tobacco confirms that the gene encodes a subunit of PSII and causes changes at the acceptor side of that assembly. Forward electron transport from the donor side occurs and appears not to be affected in Δ*psbL*. It is important to note again that the results obtained with Δ*psbL* are critically dependent on the developmental stage and the pretreatment of the material. Absence of PsbL causes instability of PSII, including PsbA, PsbE, and PsbJ (Figure 1A), and subsequent degradation of the assembly (*13*), initially without notable morphological and pigment changes of the leaf. The fraction of green leaves exhibiting relatively high residual PSII activity is low (∼10%); the amount of PsbJ parallels residual PSII activity, consistent with its role in forward electron flow. Biophysical and morphological data can be correlated and are consistent as well. It remains to be evaluated whether the preponderance of PSII monomers, observed in Δ*psbL* thylakoid lysates (*13*), is a consequence of this instability. Also, it would be interesting to see whether stationary and log-phase *Synechocystis* Δ*psbL* cultures display a similar pattern of variation.

Fm_D Fluorescence Appearance: *Possible Mechanisms.* This novel phenomenon was not reported to occur in normal nor in light stressed plants that exhibit a high Fo level, nor, to the best of our knowledge, in any other PSII mutant described so far, including Δ*psbJ* (*1*, *13*, *53*). What is the mechanism of the rise and decay of the Fm_D fluorescence that will satisfy the experimental results obtained in this work? The following possibilities can be considered: (1) The redox potential of $Q_A^{\bullet-}$:Q_A/Q_B:$Q_B^{\bullet-}$ has been altered, and reduced plastoquinone can reduce Q_A. In this case, the appearance of Fm_D was due to back electron flow from PQH_2 via Q_B to Q_A without having to cross an energy barrier. This scheme does not explain the temperature dependence of the Fm_D raise nor the thermoluminescence data showing that the redox potential of Q_A is not significantly altered in the mutant. (2) The binding affinity of the Q_B site for PQ and PQH_2 is altered in the mutant; thus, the site is progressively occupied by PQH_2 as its relative concentration increases during the light pulse. In this case, Q_A is not necessarily reduced by PQH_2. Appearance of Fm_D could have been induced by the measuring beam due to the occupancy of the Q_B site by a reduced ligand that cannot accept electrons from $Q_A^{\bullet-}$, as is the case for DCMU. While apparently this possibility fits with many of the experimental data, it does not explain the Fm_D appearance in darkness when $Q_A^{\bullet-}$ has already been partially oxidized. The intensity of the fluorescence measuring beam used in this work (PAM settings 4 at 1.6 kHz) was 0.3% of that required to reach levels close to Fm_D in the presence of DCMU and thus cannot explain the appearance of Fm_D. (3) The affinity of the Q_B site for PQ and PQH_2 has been altered without necessarily affecting redox potentials. Therefore, PQH_2 can compete with the reduced semiquinone for binding at this site allowing back electron flow to Q_A from reduced PQH_2 against an energy barrier.

The third possibility seems to be the most plausible satisfying all the experimental results, that is, the dependence of Fm_D on the accumulation of plastoquinol during the light pulse, the unaffected redox potential of Q_A, the temperature dependence of the Fm_D appearance, as well as the loss of the thermoluminescence B band emission.

Cyt b_{559} is considered as a component of PSII sensitive to structural changes of the complex (*66*−*69*). It is possible that changes in the redox potential of cyt b_{559} and/or redox coupling with Q_A may promote the recombination of $Q_A^{\bullet-}$ with $P680^{\bullet+}$ via pheophytin and circumvent recombination via tyrosine $Y_Z^{\bullet-}$ to the oxidized Mn cluster. Further work is required to test this possibility.

All results presented in Figures 2−8 are consistent with the hypothesis that Fm_D in the Δ*psbL* mutant is due to back electron flow from PQH_2 to PSII. The fluorescence rise of the Fm_D could be detected already within about less than a half second after the exciting light pulse, indicating that the plastoquinone pool was already reduced during the short illumination (Figures 1B and 6A). Blocking the reduction of plastoquinone by PSII, removing electrons from the reduced pool, or lowering the temperature abolished the appearance of Fm_D. Under anoxygenic conditions, a still higher and broader Fm_D peak appeared suggesting a delayed $Q_A^{\bullet-}$ reoxidation and thus a decreased Fm_D decay (Figure 8). The energy of activation required for the back electron flow from the PQ pool uphill on the redox potential ladder is not sufficient at the lower temperature; hence, closing PSII in darkness and the rise of the Fm_D level are prevented at low temperature in Δ*psbL*. PsbL may be involved in regulating the affinity of the Q_B site for plastosemiquinone, plastoquinone, or plastoquinol.

The relatively low content of PSII in the Δ*psbL* mutant as compared to the wild type (*13*) limits the overall electron flow and accumulation of PQH_2 in the light exposed leaves. Reduced PSII levels may not compete with plastoquinol pool oxidation upon activation of PSI and with electron transfer to artificial acceptors or with the carbon fixation sink. This also explains the absence of Fm_D in Δ*psbL* leaves illluminated with continuous white or FR light, which preferentially excites PSI (Figure 7A).

The anomalous fluorescence decay kinetics exhibited by Δ*psbL* leaves represents the sum of several partially overlapping processes. In interpreting the results, one should keep in mind that the Fm_D fluorescence is elicited by the weak modulated measuring beam, and its height is always related to the level of reduced Q_A. Depending on the duration and/or intensity of the light pulse, the reduction of Q_A and the forward electron flow may result in accumulation of reduced plastoquinone. However, this does not affect the raise and initial fast phase of Fm_L decay following pulse cessation (Figure 5). The electron flow to the PQ pool after switching off the pulse accounts for the initial fast fluorescence decay. During the light pulse, the electron flow-pressure driven by the low potentials of reduced pheophytin and Q_A relative to the plastoquinone pool prevents back electron flow from plastoquinol at 22 °C. Upon cessation of the light pulse, electron flow from the residual reduced pheophytin and Q_A populations to Q_B maintains a pressure that prevents the back reaction. However, as reduced pheophytin and $Q_A^{\bullet-}$ have been oxidized in Δ*psbL*, the electrons from the PQH_2 pool can flow backward reducing Q_A and thus generating the Fm_D peak. The extent of the $Q_A^{\bullet-}$ oxidation before appearance of the Fm_D peak in the ΔpsbL mutant is related to the ratio $Q_A^{\bullet-}/PQH_2$ (Figure 5A).

The phenomenon of back electron flow from plastoquinol and the reduction of PSII may occur also in the wild type. However, this has only been assumed to take place following harsh treatments such as high temperature (*33*−*36*) and thus may be also due to alterations of the Q_B site opening (i.e., allowing competition of PQH_2 binding to the site with PQ and possibly Q_B^-). Furthermore, the reduction of Q_A by PQH_2 may require deprotonation, a process that may require energy and could be facilitated by alterations of the Q_B site properties. The altered accessibility of the mutant Q_B site as indicated by lowering the inhibitory effect of DCMU (Figure 5) and the presence of a relatively high concentration of reduced PQH_2 accumulated during the light pulse in the membrane relative to PSII centers may facilitate the back electron flow and reduction of Q_A. Presently, considering the technical difficulties imposed by the instability of PSII, we cannot measure the binding constants or the redox state of individual components of the system.

The observation that Fm_D occasionally exceeds Fm_L is exclusively observed in leaves with very weak PSII activity. We have shown that this is due to the negative contribution of inactive centers to Fm_L. In leaves without any variable fluorescence, the light pulse induces a transient small decrease of the fluorescence that increases again and reaches the previous Fo level already at the end of the pulse (Figure 3). Therefore, the true Fm_L level is repressed during the light pulse due to the contribution of inactive centers. The less the PSII activity is in green leaves the higher the contribution of inactive centers to the reduction of Fm_L. This is the reason why Fm_D occasionally exceeds Fm_L in leaves with a low level of variable fluorescence.

Thermoluminescence signals at temperatures in the range of 25−35 °C emitted by back electron flow from the $Q_B^{\bullet-}$ semiquinone and charge recombination (*55*) could not be detected in the Δ*psbL* mutant leaves. Excitation of intact leaves above the freezing temperature induces a 43−45 °C emission in Δ*psbL* and also in control leaves. The thermoluminescence band at this temperature is still a matter of dispute. The so-called C band in this range has been attributed to recombination of the charge pair $Tyr^{\bullet+}/Q_A^{\bullet-}$ in PSII*β* (Q_B nonreducing centers) and Ca^{2+} depleted PSII and seems to be independent of the S-states of the manganese cluster (*69*−*73*). At 43 °C, the afterglow band appears as well, which is missing in DCMU treated wild type leaves but found in treated mutant material (Figure 9) again supporting that the Q_B site is altered in the mutant. This band oscillates with the number of excitation flashes (*74*, *75*) and has been attributed to the back flow of electrons from enhanced heat induced reduction of PQH_2, rebinding to the Q_B site and $S_{2,3}/Q_A^{\bullet-}$ charge recombination. Exchange of $Q_B^{\bullet-}$ formed during the saturating pulse with PQ from the pool can explain the absence of the thermoluminescence B band when Δ*psbL* leaves are excited at about 1 °C. In this case, electrons will be drained from reduced Q_A toward the PQ pool, prevent back reaction, and account also for the fast decay of the Fm_L fluorescence and absence of Fm_D at this temperature (Figure 4B).

Reduction of Q_A or Q_B sites in darkness by PQH_2 was demonstrated to occur in plants pretreated severely by heat and relatively strong light (*24*, *25*, *29*). Increase in chlorophyll *a* fluorescence in darkness has also been reported to occur although at a much lower extent after longer applications of actinic light to wild type plants (*33*−*36*). The fluorescence in these cases reached the maximum after about 30 s and could only partially be quenched by FR light. This

is in contrast to the Fm_D exhibited by the Δ*psbL* mutant because (1) the Fm_D appeared already after application of a single light pulse but not after a longer actinic illumination; (2) Fm_D appeared after about 4−6 s; (3) Fm_D was completely reversible by application of FR light in the *psbL* mutant; and (4) the Fm_D increase was related to the reduction of plastoquinone by electron flow from PSII.

In several *Arabidopsis* mutants (*76*) and in a tobacco *psbF* mutant (*77*), the fluorescence increase in the dark after switching off actinic light was not reversible. This fluorescence increase was due to a substantial quenching below the initial Fo fluorescence level during the actinic illumination. We have found that this quenching is due to the high energy quenching and not due to quinone reduction since nigericine abolished the phenomenon and FR light had no effect on the fluorescence increase (*78*).

Physiological Significance of Ensuring Forward Electron Transport. The results of this work demonstrate that PsbL is not required for the assembly of a functional PSII that can perform charge separation/recombination, water oxidation, and electron flow via the Q_A and Q_B sites to reduce plastoquinone. However, in the absence of PsbL, the Q_B site properties are altered allowing return of electrons from PQH_2 to the Q_A site. Electron flow within the PSII assembly is a reversible process, regulated by the redox potential gaps between electron carriers that promote forward electron flow from the excited primary donor, P680*, via bound Q_A to the bound Q_B site. Return of electrons uphill on the potential ladder occurs only from reduced semiquinone by supply of energy (heat) and competes with forward flow to the plastoquinone pool (*23*, *79*). This ensures that the energy absorbed by the photochemical center and utilized for charge separation is not wasted in a futile cycle. Back flow of electrons from the reduced PQH_2 pool to Q_A is prevented by secluding the bound quinone Q_B in a special pocket formed by the D1 protein (*80*). This site has a higher affinity for the oxidized than for the reduced plastoquinone, which is released by the one-way gate opening upon double reduction of the bound molecule (*23*). This feature of the Q_B site gating system ensures that the plastoquinol redox state is not communicated to the core of PSII. Partial reduction of the PQ pool should not cause reduction of the acceptor side of PSII, which may block forward electron flow and promote back electron flow and charge recombination, the source of oxidative stress and inactivation of PSII even under weak light conditions (*57*, *81*).

In this context, it is noteworthy that the inactivation of *PsbJ* encoding another low molecular mass component of PSII significantly lowers the forward electron flow from $Q_A^{\bullet-}$ to the PQ pool and promotes back electron flow within PSII (*1*). The low temperature effect on back electron flow to PSII clearly demonstrated that energy is required to reduce or reoxidize Q_A in Δ*psbL* or Δ*psbJ*, respectively. Thus, the PsbL and PsbJ proteins act to regulate the communication between PSII and photosynthetic electron-transfer chain.

ACKNOWLEDGMENT

We are grateful to Martina Reimers for skilfull technical assistance. We thank Lina Lezhneva for critical reading of the manuscript and Dr. Anja Krieger-Liszkay for discussing the results.

REFERENCES

1. Regel, R. E., Ivleva, N. B., Zer, H., Meurer, J., Shestakov, S. V., Herrmann, R. G., Pakrasi, H. B., and Ohad, I. (2001) Deregulation of electron flow within photosystem II in the absence of the PsbJ protein, *J. Biol. Chem. 276*, 41473−41478.
2. Diner, B. A., and Rappaport, F. (2002) Structure, dynamics, and energetics of the primary photochemistry of photosystem II of oxygenic photosynthesis, *Annu. Rev. Plant Physiol. Plant Mol. Biol. 53*, 551−580.
3. Boekema, E. J., Hankamer, B., Bald, D., Kruip, J., Nield, J., Boonstra, A. F., Barber, J., and Rögner, M. (1995) Supramolecular structure of the photosystem II complex from green plants and cyanobacteria, *Proc. Natl. Acad. Sci. U.S.A. 92*, 175−179.
4. Barber, J., and Kühlbrandt, W. (1999) Photosystem II, *Curr. Opin. Struct. Biol. 9*, 469−475.
5. Nield, J., Orlova, E. V., Morris, E. P., Gowen, B., van Heel, M., and Barber, J. (2000) 3-D map of the plant photosystem II supercomplex obtained by cryoelectron microscopy and single particle analysis, *Nat. Struct. Biol. 7*, 44−47.
6. Hankamer, B., Morris, E., Nield, J., Carne, A., and Barber, J. (2001) Subunit positioning and transmembrane helix organization in the core dimer of photosystem II, *FEBS Lett. 504*, 142−151.
7. Kashino, Y., Lauber, W. M., Carroll, J. A., Wang, Q., Whitmarsh, J., Satoh, K., and Pakrasi, H. B. (2002) Proteomic analysis of a highly active photosystem II preparation from the cyanobacterium *Synechocystis sp.* PCC 6803 reveals the presence of novel polypeptides, *Biochemistry 41*, 8004−8012.
8. Kamiya, N., and Shen, J. R. (2003) Crystal structure of oxygen-evolving photosystem II from *Thermosynechococcus vulcanus* at 3.7 Å resolution, *Proc. Natl. Acad. Sci. U.S.A. 100*, 98−103.
9. Morris, E. P., Hankamer, B., Zheleva, D., Friso, G., and Barber, J. (1997) The three-dimensional structure of a photosystem II core complex determined by electron crystallography, *Structure 5*, 837−849.
10. Rhee, K. H., Morris, E. P., Barber, J., and Kühlbrandt, W. (1998) Three-dimensional structure of the plant photosystem II reaction centre at 8 Å resolution, *Nature 396*, 283−286.
11. Barber, J., and Nield, J. (2002) Organization of transmembrane helices in photosystem II: comparison of plants and cyanobacteria, *Philos. Trans. R. Soc. London, Ser. B 357*, 1329−1335.
12. Hankamer, B., Morris, E., Nield, J., Gerle, C., and Barber, J. (2001) Three-dimensional structure of the photosystem II core dimer of higher plants determined by electron microscopy, *J. Struct. Biol. 135*, 262−269.
13. Swiatek, M., Regel, R. E., Meurer, J., Wanner, G., Pakrasi, H. B., Ohad, I., and Herrmann, R. G. (2003) Effects of selective inactivation of individual genes for low-molecular-mass subunits on the assembly of photosystem II, as revealed by chloroplast transformation: the *psbEFLJ* operon in *Nicotiana tabacum*, *Mol. Genet. Genomics 268*, 699−710.
14. Morais, F., Kühn, K., Stewart, D. H., Barber, J., Brudvig, G. W., and Nixon, P. J. (2001) Photosynthetic water oxidation in cytochrome *b*(559) mutants containing a disrupted heme-binding pocket, *J. Biol. Chem. 276*, 31986−31993.
15. Diner, B. A., and Babcock, G. T. (1996) Structure, dynamics, and energy conversion efficiency in photosystem II, in *Oxygenic Photosynthesis: The Light Reactions* (Ort, D. R., Yocum, C. F., Eds.) pp 213−247, Kluwer Academic Publishers, Dordrecht, The Netherlands.
16. Debus, R. J. (1992) The manganese and calcium ions of photosynthetic oxygen evolution, *Biochim. Biophys. Acta 1102*, 269−352.
17. Debus, R. J. (2000) The polypeptides of photosystem II and their influence on manganotyrosyl-based oxygen evolution, *Met. Ions. Biol. Syst. 37*, 657−711.
18. Velthuys, B. R. (1981) Electron dependent competition between plastoquinone and inhibtors for binding to photosystem II, *FEBS Lett. 12*, 277−281.
19. Okamura, M. Y., and Feher, G. (1992) Proton transfer in reaction centers from photosynthetic bacteria, *Annu. Rev. Biochem. 61*, 861−896.
20. Trebst, A. (1986) The topology of the plastoquinone and herbicide binding peptides of photosystem II in the thylakoid membrane, *Z. Naturforsch. 41c*, 240−245.

21. Mäenpää, P., Miranda, T., Tyystjærvi, E., Tyystjærvi, T., Govindjee, Ducruet, J. M., Etienne, A. L., and Kirilovsky, D. A. (1995) Mutation in the D-de Loop of D1 Modifies the stability of the S_2Q_A and S_2Q_B States in Photosystem II, *Plant Physiol. 107*, 187−197.
22. Govindjee (1990) Photosystem II heterogeneity: the acceptor side, *Photos. Res. 25*, 151−160.
23. Stowell, M. H., McPhillips, T. M., Rees, D. C., Soltis, S. M., Abresch, E., and Feher, G. (1997) Light-induced structural changes in photosynthetic reaction center: implications for mechanism of electron−proton transfer, *Science 276*, 812−816.
24. Groom, Q., Kramer, D. M., Crofts, A. R., and Ort, D. R. (1993) The nonphotochemical reduction of plastoquinone in leaves, *Photos. Res. 36*, 205−215.
25. Feild, T. S., Nedbal, L., and Ort, D. R. (1998) Nonphotochemical reduction of the plastoquinone pool in sunflower leaves originates from chlororespiration, *Plant Physiol. 116*, 1209−1218.
26. Krause, G. H., and Weis, E. (1984) Chlorophyll fluorescence as a tool in plant physiology. II. Interpretation of fluorescence signals, *Photosynth. Res. 5*, 139−157.
27. Krause, G. H., and Weis, E. (1991) Chlorophyll fluorescence and photosynthesis: The basics, *Annu. Rev. Plant Physiol. Plant Mol. Biol. 42*, 313−349.
28. Cao, J., and Govindjee (1990) Chlorophyll a fluorescence transient as an indicator of active and inactive Photosystem II in thylakoid membranes, *Biochim. Biophys. Acta 1015*, 180−188.
29. Havaux, M. (1996) Short-term responses of photosystem I to heat stress. Induction of a PSII-independent electron transport through PSI fed by stromal components, *Photos. Res. 47*, 85−97.
30. Sazanov, L. A., Burrows, P. A., and Nixon, P. J. (1998) The chloroplast Ndh complex mediates the dark reduction of the plastoquinone pool in response to heat stress in tobacco leaves, *FEBS Lett. 429*, 115−118.
31. Yamane, Y., Shikanai, T., Kashino, Y., Koike, H., and Satoh, K. (2000) Reduction of Q(A) in the dark: Another cause of fluorescence $F - o$ increases by high temperatures in higher plants, *Photos. Res. 63*, 23−34.
32. Bukhov, N. G., Samson, G., and Carpentier, R. (2000) Non-photosynthetic reduction of the intersystem electron transport chain of chloroplasts following heat stress. Steady-state rate, *Photochem. Photobiol. 72*, 351−357.
33. Asada, K., Heber, U., and Schreiber, U. (1993) Electron flow to the intersystem chain from stromal components and cyclic electron flow in maize chloroplasts, as detected in intact leaves by monitoring redox change of P700 and chlorophyll fluorescence, *Plant Cell Physiol. 34*, 39−50.
34. Mano, J., Miyake, C., Schreiber, U., and Asada, K. (1995) Photoactivation of the electron flow from NADPH to plastoquinone in spinach chloroplasts, *Plant Cell Physiol. 36*, 1589−1598.
35. Burrows, P. A., Sazanov, L. A., Svab, Z., Maliga, P., and Nixon, P. J. (1998) Identification of a functional respiratory complex in chloroplasts through analysis of tobacco mutants containing disrupted plastid *ndh* genes, *EMBO J. 17*, 868−876.
36. Shikanai, T., Endo, T., Hashimoto, T., Yamada, Y., Asada, K., and Yokota, A. (1998) Directed disruption of the tobacco *ndhB* gene impairs cyclic electron flow around photosystem I, *Proc. Natl. Acad. Sci. U.S.A. 95*, 9705−9709.
37. Shinozaki, K., Ohme, M., Tanaka, M., Wakasugi, T., Hayashida, N., Matsubayashi, T., Zaita, N., Chunwongse, J., Obokata, J., Yamaguchi-Shinozaki, K., Ohto, C., Torazawa, K., Meng, B., Sugita, M., Deno, H., Kamogashira, T., Yamada, K., Kusuda, J., Takaiwa, F., Kato, A., Tohdoh, N., Shimada, H., and Sugiura, M. (1986) The complete nucleotide sequence of the tobacco chloroplast genome: its gene organization and expression, *EMBO J. 5*, 2043−2049.
38. Pakrasi, H. B., Nyhus, K. J., and Granok, H. (1990) Targeted deletion mutagenesis of the beta subunit of cytochrome b_{559} protein destabilizes the reaction center of photosystem II, *Z. Naturforsch. C 45*, 423−429.
39. Morais, F., Barber, J., and Nixon, P. J. (1998) The chloroplast-encoded alpha subunit of cytochrome b_{559} is required for assembly of the photosystem two complex in both the light and in the dark in *Chlamydomonas reinhardtii*, *J. Biol. Chem. 273*, 29315−29320.
40. Barber, J., and De Las Rivas, J. (1993) A functional model for the role of cytochrome b_{559} in the protection against donor and acceptor side photoinhibition, *Proc. Natl. Acad. Sci. U.S.A. 90*, 10942−10946.
41. Whitmarsh, J., Samson, G., and Poulson, M. (1994) in *Photoinhibition of Photosynthesis* (Baker, N. R., Bowyer, J. R., Eds.) pp 75−93, BIOS Scientific Publishers Ltd., Oxford.
42. Poulson, M., Samson, G., and Whitmarsh, J. (1995) Evidence that cytochrome b_{559} protects photosystem II against photoinhibition, *Biochemistry 34*, 10932−10938.
43. Stewart, D. H., and Brudvig, G. W. (1998) Cytochrome b_{559} of photosystem II, *Biochim. Biophys. Acta 1367*, 63−87.
44. Kruk, J., and Strzalka, K. (2001) Redox changes of cytochrome b_{559} in the presence of plastoquinones, *J. Biol. Chem. 276*, 86−91.
45. Buser, C. A., Diner, B. A., and Brudvig, G. W. (1992) Photooxidation of cytochrome b_{559} in oxygen-evolving photosystem II, *Biochemistry 31*, 11449−11459.
46. Whitmarsh, J., and Pakrasi, H. B. (1996) in *Oxygenic Photosynthesis*: The Light Reactions (Ort, D. R., Yocum, C. F., Eds.) pp 249−264, Kluwer Academic Publishers, Norwell, MA.
47. Ikeuchi, M., Koike, H., and Inoue, Y. (1989) N-terminal sequencing of low-molecular-mass components in cyanobacterial photosystem II core complex. Two components correspond to unidentified open reading frames of plant chloroplast DNA, *FEBS Lett. 253*, 178−182.
48. Nagatsuka, T., Fukuhara, S., Akabori, K., and Toyoshima, Y. (1991) Disintegration and reconstitution if photosystem II reaction center core complex II. Possible involvement of low-molecular-mass proteins in the functioning of Q_A in the PSII reaction center, *Biochim. Biophys. Acta 1057*, 223−231.
49. Kitamura, K., Ozawa, S., Shiina, T., and Toyoshima, Y. (1994) L protein, encoded by psbL, restores normal functioning of the primary quinone acceptor, Q_A, in isolated D1/D2/CP47/Cytb_{559}/I photosystem II reaction center core complex, *FEBS Lett. 354*, 113−116.
50. Ozawa, S., Kobayashi, T., Sugiyama, R., Hoshida, H., Shiina, T., and Toyoshima, Y. (1997) Role of PSII-L protein (*psbL* gene product) on the electron transfer in photosystem II complex. 1. Over-production of wild type and mutant versions of PSII-L protein and reconstitution into the PSII core complex, *Plant Mol. Biol. 34*, 151−161.
51. Hoshida, H., Sugiyama, R., Nakano, Y., Shiina, T., and Toyoshima, Y. (1997) Electron paramagnetic resonance and mutational analyses revealed the involvement of photosystem II-L subunit in the oxidation step of Tyr-Z by P680+ to form the Tyr-Z+P680Pheo− state in photosystem II, *Biochemistry 36*, 12053−12061.
52. Anbudurai, P. R., and Pakrasi, H. B. (1993) Mutational analysis of the PsbL protein of photosystem II in the cyanobacterium *Synechocystis* sp. PCC 6803, *Z. Naturforsch. C 48*, 267−274.
53. Hager, M., Hermann, M., Biehler, K., Krieger-Liszkay, A., and Bock, R. (2001) Lack of the small plastid-encoded PsbJ polypeptide results in a defective water-splitting apparatus of photosystem II, reduced photosystem I levels, and hypersensitivity to light, *J. Biol. Chem. 277*, 14031−14039.
54. Schreiber, U., and Krieger, A. (1996) Two fundamentally different types of variable chlorophyll fluorescence in vivo, *FEBS Lett. 397*, 131−135.
55. Rutherford, A. W., Crofts, A. R., and Inoué, Y. (1982) Thermoluminescence as a probe of photosystem II photochemistry. The origin of the flash-induced glow peaks, *Biochim. Biophys. Acta 682*, 457−465.
56. Vass, I., and Govindjee (1996) Thermoluminescence from the photosynthetic apparatus, *Photos. Res. 48*, 117−126.
57. Zer, H., Prasil, O., and Ohad, I. (1994) Role of plastoquinol oxidoreduction in regulation of photochemical reaction center II-D1 protein turnover in vivo, *J. Biol. Chem. 269*, 17670−17676.
58. Klughammer, C., and Schreiber, U. (1994) An improved method, using saturating light pulses, for the determination of photosystem I quantum yield via P700+-absorbance changes at 830 nm, *Planta 192*, 261−268.
59. Prasil, O., Adir, N., and Ohad, I. (1991) Dynamics of Photosystem II: Mechanism of Photoinhibition and recovery in vivo, in *Topics in Photosynthesis* (Barber, J., Ed.) Vol. 11, pp 295−348, Elsevier Publishers B. V., Amsterdam, The Netherlands.
60. Rutherford, A. W., Govindjee, and Inoué, Y. (1984) Charge accumulation and photochemistry in leaves studied by thermoluminescence and delayed light emission, *Proc. Natl. Acad. Sci. U.S.A. 81*, 1107−1111.
61. Sane, P. V., and Rutherford, A. W. (1986) Thermoluminescence from photosynthetic membranes, in *Light Emission in Plants and*

Bacteria. (Govindjee, Amesz, J., and Fork, D. C., Eds.) pp 329−361, Academic Press, New York.
62. Vass, I., and Inoué, Y. (1992) Thermoluminescence in the study of photosystem II, in *The Photosystems: Structure, Function and Molecular Biology* (Barber, J., Ed.) pp 259−294, Elsevier, Amsterdam, The Netherlands.
63. Rutherford, A. W., Renger, G., Koike, H., and Inoué, Y. (1984) Thermoluminescence as a probe of photosystem II. The redox and protonation states of the secondary acceptor quinone and the oxygen evolving enzyme, *Biochim. Biophys. Acta 767*, 548−556.
64. Miranda, T., and Ducruet, J. M. (1995) Characterization of the chlorophyll thermoluminescence afterglow in dark-adapted or far-red-illuminated plant leaves, *Plant Physiol. Biochem. 33*, 689−699.
65. Demeter, S., Goussias, C., Bernát, G., Kovács, L., and Petrouleas, V. (1993) Participation of the $g = 1.9$ and $g = 1.82$ EPR forms of the semiquinone−iron complex, $Q_A^{\bullet -}Fe^{2+}$ of photosystem II in the generation of the Q and C thermoluminescence bands, respectively, *FEBS Lett. 336*, 352−356.
66. Vrettos, J. S., Stewart, D. H., de Paula, J. C., and Brudvig, G. W. (1999) Low-temperature optical and resonance Raman spectra of a carotenoid cation radical in photosystem II. *J. Phys. Chem. B 103*, 6403−6406.
67. Mizusawa, N., Yamashita, T., and Miyao, M. (1999) Restoration of the high-potential form of cytochrome b_{559} of photosystem II occurs via a two-step mechanism under illumination in the presence of manganese ions, *Biochim. Biophys. Acta*. *1410*, 273−286.
68. Krieger, A., Rutherford, W., and Johnson, G. N. (1995) On the determination of redox midpoint potential of the primary quinone electron acceptor, QA, in Photosystem II, *Biochim. Biophys. Acta 1229*, 193−201
69. Inoué, Y., Ichikawa, T., and Shibata, K. (1976) Development of thermoluminescence bands during greening of wheat leaves under continuous and intermittent illumination, *Photochem. Photobiol. 23*, 125−130.
70. Ono, T., and Inoué, Y. (1989) Removal of Ca by pH 3.0 treatment inhibits S2 to S3 transition in photosynthetic oxygen evolving system, *Biochim. Biophys. Acta 973*, 443−449.
71. Krieger, A., Weis, E., and Demeter, S. (1993) Low pH induced Ca^{2+} ion release in the water-splitting system is accompanied by a shift in the midpoint redox potential of the primary quinone acceptor Q_A, *Biochim. Biophys. Acta 1144*, 411−418.
72. Johnson, G. N., Boussac, A., and Rutherford, A. W. (1994) The origin of the 40−50 °C thermoluminescence band in photosystem II, *Biochim. Biophys. Acta 1184*, 85−92.
73. Andrée, S., Weis, E., and Krieger, A. (1998) Heterogeneity and photoinhibition of photosystem II studied with thermoluminescence, *Plant Physiol. 116*, 1053−1061.
74. Janda, T., Szalai G., Giauffret, C., Páldi, E., and Ducruet, J. M. (1999) The thermoluminescence afterglow band as a sensitive indicator of abiotic stresses in plants, *Z. Naturforsch. C 54*, 629−633.
75. Krieger, A., Bolte, S., Dietz, K. J., and Ducruet, J. M. (1998) Thermoluminescence studies on the facultative crassulacean-acid-metabolism plant *Mesembryanthemum crystallinum* L, *Planta 205*, 587−594.
76. Meurer, J., Meierhoff, K., Westhoff, P. (1996) Isolation of high-chlorophyll-fluorescence mutants of *Arabidopsis thaliana* and their characterisation by spectroscopy, immunoblotting, and Northern hybridization, *Planta 198*, 385−396.
77. Bondarava, N., De Pascalis, L., Al-Babili, S., Goussias, C., Golecki, J. R., Beyer, P., Bock, R., and Krieger-Liszkay, A. (2003) Evidence that cytochrome b_{559} mediates the oxidation of reduced plastoquinone in the dark, *J. Biol. Chem. 278*, 13554−13560.
78. Dal Bosco, C., Lezhneva, L., Biehl, A., Leister, D., Strotmann, H., Wanner, G., Meurer, J. (2004) Inactivation of the chloroplast ATP synthase gamma subunit results in high nonphotochemical fluorescence quenching and altered nuclear gene expression in *Arabidopsis thaliana*, *J. Biol. Chem. 278*, 1060−1068.
79. Bowes, J. M., and Crofts, A. R. (1980) Binary oscillations in the rate of reoxidation of the primary acceptor of photosystem II, *Biochim. Biophys. Acta 590*, 3733−3784.
80. Nixon, P. J., Komenda, J., Barber, J., Deak, Z., Vass, I., and Diner, B. A. (1995) Deletion of the PEST-like region of photosystem II modifies the Q_B-binding pocket but does not prevent rapid turnover of D1, *J. Biol. Chem. 270*, 14919−14927.
81. Keren, N., Gong, H., and Ohad, I. (1995) Oscillations of reaction center II-D1 protein degradation in vivo induced by repetitive light flashes. Correlation between the level of RCII-Q_B- and protein degradation in low light, *J. Biol. Chem. 270*, 806−814.

BI0348260